Out-of-Plane Cyclic Response of Masonry Infilled RC Frames: An Experimental Study

Filip Anić[a], Davorin Penava[*a], Ivica Guljaš[a], Vasilis Sarhosis[b]

[a] *Faculty of Civil engineering and Architecture Osijek, Josip Juraj Strossmayer University of Osijek*
[b] *Faculty of Engineering and Physical Sciences, School of Civil Engineering, University of Leeds*

Abstract

This paper presents the development of an experimental campaign to investigate the cyclic out-of-plane response of reinforced concrete frames containing masonry infill walls using non-contact optical techniques able to measure contour strains and deformations. Bare RC frames as well as fully infilled walls with and without window and door openings were tested in the laboratory. From the results analysis, it was found that neither the infill walls nor the openings significantly affected the overall behaviour of specimens. However, the infill walls suffered substantial damage in the range of 1.25 -2.50 % storey drift ratio which pose a risk to life and livelihoods. Also, it was found that masonry walls containing openings accumulated further damage, especially these with eccentrically positioned ones, when compared to the fully infilled frames. Finally, for masonry infills containing openings and when debonding of the infill from the surrounding frame occurs, parts of infill walls could fall out due to inertia and render the overall combined in-plane behaviour of the specimen.

Keywords: out-of-plane response, masonry infilled rc frames, door and window openings, inter-storey drift force method; vision based remote sensing

1. Introduction

Structural systems of multi-storey buildings are composed of reinforced concrete (RC) or structural steel frames containing infill walls with or without openings. Within that system, the infill wall is considered as a non-structural component, while the frame is considered as a structural one. When these structures are excited by dynamical actions, such as earthquake events, the infill interacts with the surrounding frame and affects the overall stiffness, strength and overall ductility of the structure. Although the aforementioned phenomenon was known since 1930's [1], our current seismic design codes (e.g. Eurocode 8 [2]) does not take into account the interaction of the masonry infill with the surrounding frame due to due to lack of research in the area.

Over the last three decades, several researchers from the fields of blast engineering, structural dynamics and seismic engineering undertook systematic experimental and numerical studies to understand the interaction effects between frames and infills [3,4] and [5,6]. From these studies, it became apparent that the interaction between the structural frame and the masonry infill walls can be: a) In-plane (IP); b) Out-of-plane (OoP); and c). Combined IP+OoP. Figure 1 is a Venn diagram showing the relationship between the research on the interaction between frame and masonry infill walls as shared between different fields of research over the last 30 years. Circles that overlap present investigations with common research interest. Also, circles are not to scale.

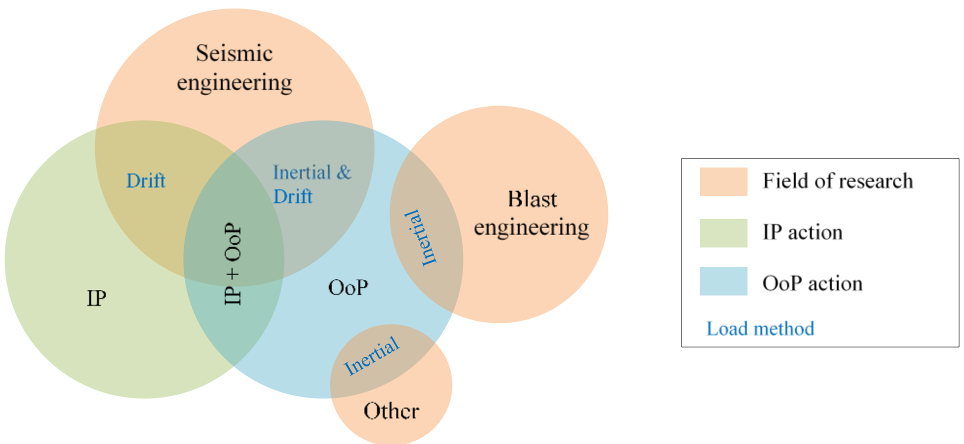

Figure 1. Research on the interaction between frame and masonry infill walls as shared between different fields (circles not in scale)

---

* Corresponding author;
e-mail addresses: davorin.penava@gfos.hr (Davorin Penava)

Now, from the principles of earthquake engineering, it is well known that seismic actions result in inter-storey drift and inertial forces. Inter-storey drift is the consequence of rigid diaphragm movement during earthquake shaking. Also, inertial forces are acting on the frames and masonry infill members, are opposite in direction to the accelerating force induced by the earthquake and are equal to the product of the accelerating force and the mass of the structural members. Also, the inertial forces are dominant in the upper part of the structure, while the inter-storey drift forces are dominant in the lower storeys. To reflect such phenomena in an experimental set up, the inter-storey drift forces could be represented by concentrated loads applied directly onto the frame, while the inertial forces, via infill wall pressurizing systems such as airbags. From past research, it was found that there are several experimental tests on masonry infill walls subjected to IP inter-storey drifts, while experimental tests on masonry infill wall panels subjected OoP inter-storey drift forces are limited. In fact, only [7,8] performed experimental tests on infilled frames with inter-storey drift forces in the OoP direction. This adds up to about 7% of the OoP field of research, in contrast to inertial and dynamical tests which take up to 70 and 26 % respectively [9]. Also, both researchers performed their OoP drift force investigations as a part of combined IP and OoP loads on structural steel frames.

Experimental studies on masonry infill walls subjected to OoP inertial forces were initially undertaken in the 1950's funded through USA Air Force in the subject area of blast engineering [3,10]. The blast wave from the explosion pressurises the load-bearing wall. To simulate the blast wave in controllable, i.e. laboratory conditions, use of airbags was introduced. The airbag was placed between the reaction wall and the masonry infill wall. Then, the airbag was inflated and pressurised the wall to mimic the blast wave or accelerated masses from a blast. Afterwards, researchers from the field of seismic engineering acquired the same method to study the out of plane behaviour of masonry infill frames when subjected to earthquake loads [11]. The infill walls were pressurised, while the frames were restrained from movement. Usually, the monitoring points for observing displacements were set up across the infill wall in either cross or eight-pointed star pattern. Also, at that time, optics to measure displacements were used, e.g. [12]. One of the main findings derived from such experimental tests was the concept of "arching action". In detail, McDowell [3] found that infill wall cracks and clamps at its supports. Thus, the infill wall develops the same mechanism as a three-hinged arch, i.e. resisting transversal thought normal forces. Later, numerous experiments on masonry infill wall panels were conducted and their main findings are:

a) The OoP behaviour is highly dependent on restrain conditions. Reduction in restrain conditions reduces the load-bearing capacity, failure mode and in some cases deformation capabilities;

b) Masonry infill wall panels subjected to OoP loading with existing IP damage showed reduction of load-bearing capabilities [13–15]. However, masonry infill walls subjected to simultaneous IP and OoP load showed remarkably high stability even though heavy damage was observed [7,16], which could be attributed to wedging effects. Furthermore, it was reported that previous OoP damage profoundly affected the IP behaviour [7];

c) Vertical precompression (which represent gravity loads in real structure) was only introduced in columns, however, two research teams had different observations. One observed that the stiffness was affected up to the point where vertical precompression was overcomed by transversal forces [17]. However, the other team observed changes in crack patterns and post-peak behaviour [18];

d) The contribution of the frame on the overall behaviour is still debatable. From one hand, research undertaken by [19,20] suggests that it could affect the overall behaviour concerning frames torsional capabilities (e.g. steel vs. RC frames). On the other hand, [14] suggests that there is no to little effect;

e) The effect of openings on the overall stability is still not well investigated. Today, there are no systematic studies that address the effects of openings, and in particularly on the OoP capacity.

As aforementioned, the OoP drift driven test had only two experimental campaigns that date back to 1998's. Both of them were used for combined IP and OoP load study. Two methods were performed based on deformed shapes; one was cantilever and the other was the beam defamation shape [7] (Fig. 2). Both of them represent various orthogonal IP lateral load resisting elements. It was concluded that the IP behaviour was not significantly affected by such a loading type and that failure occurred at the frame rather than at the infill. The maximum displacement of the frames was 33 mm, which translates to a 1.7 % drift ratio. Furthermore, it was observed that cracks occur mainly as de-bonding of bedjoints for the cantilever case, while in the beam-loading system also with some headjoint separations.

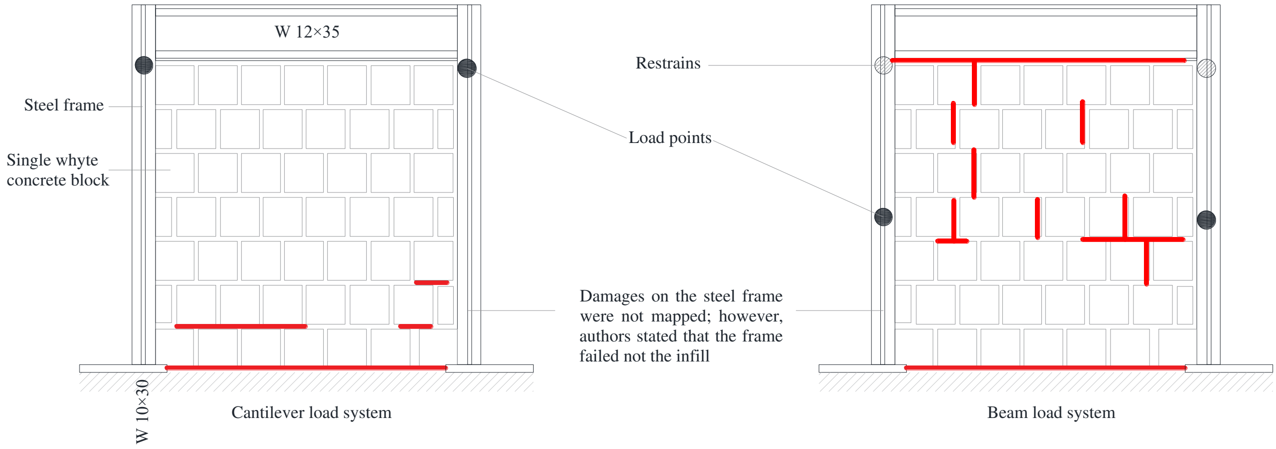

Figure 2. OoP inter-storey drift driven test [21]

By comparing inertial and drift driven tests, it is clear that they are opposites; whereas with inertial forces i.e. airbag test, the frame is intact and the infill wall damaged. The opposite is true for the drift driven test. When compared to dynamic tests, both load methods have their similarities, while the inter-storey drift method having more of them. This can be handed to the fact that most dynamical tests were done on single storey structures where inertial are lower when compared to inter-storey drift forces. For further information on this discussion, the reader can refer to [9,22]. From the above, the inter-storey drift force method was overlooked in the OoP field of research.

The aim of this paper is to present the experimental campain undertaken at the "Vladimir Sigmund Laboratory for Experimental Mechanics" within the Faculty of Civil Engineering and Architecture Osijek in which RC frames with unreinforced clay masonry infill walls were tested by unidirectional cyclic, quasi-static drift loads. The infill walls were tested with and without the presence of openings. During the experiments, full-field, non-contact optical technique was used to measure displacements and strains on the walls.

2. Materials, specimens, and experimental setup

The experimental testing presented in this paper forms part of a larger campaign performed at the Faculty of Civil Engineering and Architecture Osijek and shown in Table 1. Outcomes of the first part of this experimental campaign are presented at [23] [24]. The specimens were scaled to a 1:2.5 ratio and were designed according to EN 1998-1-1 provisions [2] having medium ductility class (DCM). Hollow clay masonry blocks, which were used as infill units, were classified as Group II by the EN 1996-1-1 [25] provisions. The general-purpose mortar was used to bond blocks and was classified as M5 class mortar by EN 1996-1-1 [25] provisions. Their mechanical properties are listed in Table 2. Frames rebar design and specimen's general geometrical properties are presented in Figure 3.

Table 1. Geometrical characteristics of tested specimens

Model mark	Appearance of the specimen	Opening	
		Type and area	Position
CD	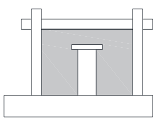	Door l_o / h_o = 0.35 / 0.90 m A_o = 0.32 m^2 A_o / A_i = 0.14	Centric e_o = l_i / 2 = 0.90 m
CW	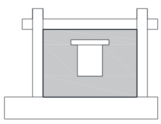	Window l_o / h_o = 50.0 / 60.0 cm A_o = 0.30 m^2 A_o / A_i = 0.13	Centric e_o = l_i / 2 = 0.90 m P = 0.40 m
ED	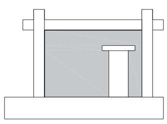	Door l_o / h_o = 0.35 / 0.90 m A_o = 0.32 m^2 A_o / A_i = 0.14	Eccentric e_o = h_i / 5 + l_o / 2 = 0.44 m

EW	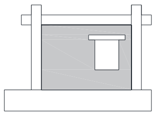	Window l_o / h_o = 50.0 / 60.0 cm A_o = 0.30 m^2 A_o / A_i = 0.13	Eccentric $e_o = h_i / 5 + l_o / 2 = 0.44$ m P = 0.40 m
BF	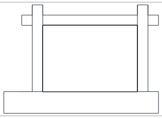	Bare frame	
FI	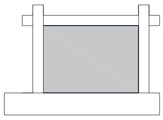	Full infill	

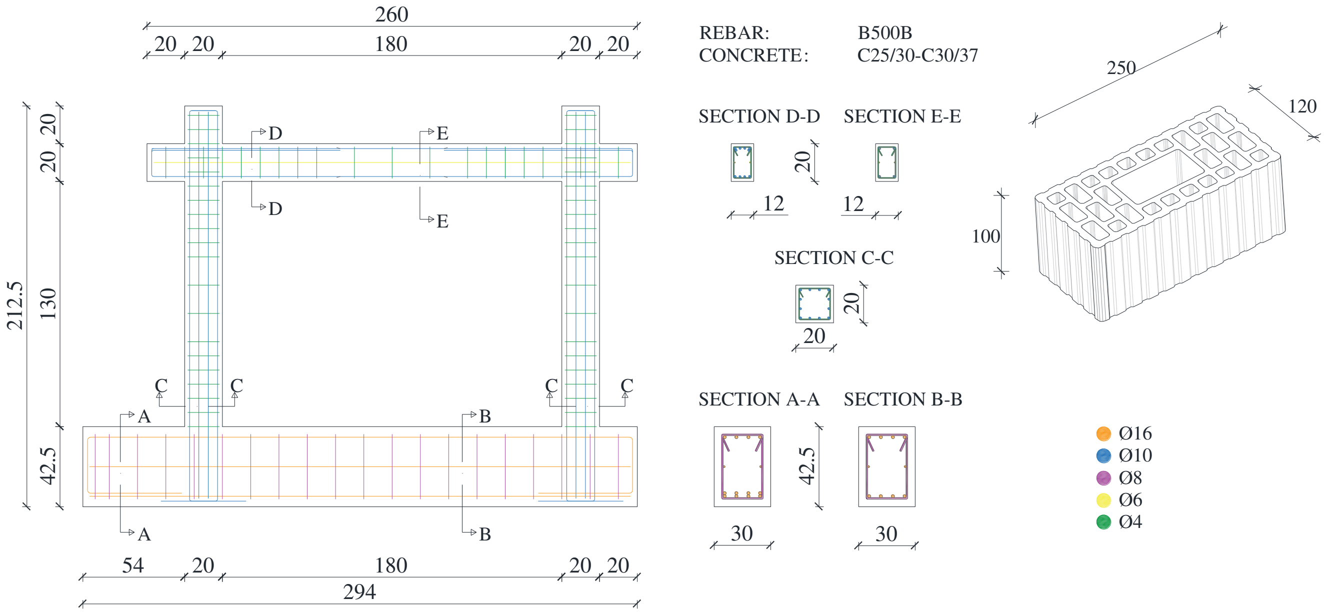

Figure 3. Rebar design and infill wall block unit geometry

This test series included OoP cyclic, quasi-static drift forces loaded upon the frame. However; prior to tests, infill walls were removed, frames were repaired (Fig. 4a) and finally infill walls were reconstructed (Fig. 4b). Afterwards, the specimens were painted white and dotted black on the front side for the optic measuring systems (Fig. 4c).


a) Repairs done on the frame b) Reconstruction of the infill wall c) Specimen painted and dotted

Figure 4. Preparation of the specimens for the second series of testing

For the repairs of the concrete frame, cracks and loose parts were removed, cleaned and the surface of the RC elements roughen. Afterwards, a fibre-reinforced, sulphate-resistant thixotropic mortar Mapegrout T60 was applied. The mortar was classified by BS EN 1504-3 provisions [26] as class R4 structural mortar.

Table 2. Mechanical properties of tested specimens

Specimen	Mechanical property	Value	Unit
Clay block [23]	Compressive strength ∥ voids	15.90	MPa
	Compressive strength ⊥ voids	2.60	MPa
Concrete (frame) [23]	Compressive strength	45.20	MPa
Mortar [23]	Mortars compressive strength	5.15	MPa
	Mortars flexural strength	1.27	MPa
Wall specimen [23]	Characteristic compressive strength	2.70	MPa
	Elastic modulus	3.90	GPa
	Ultimate strain	0.58	‰
	Initial shear strength	0.35	MPa
	Friction coefficient	0.24	-
Wall specimens OoP bending [27]	Flexural strength ∥ to bedjoints	0.21	MPa
	Flexural strength ∥ to headjoints	0.36	MPa

The OoP test setup is showed in Figure 5 and discussed here. The components from Figure 5a will be referenced thought brackets (#). The frame was placed brace-width apparat of the reaction wall; onto which, two hydraulic presses (7) and linear variable differential transducer (LVDTs) were placed (8). To ensure the hydraulic press (7) is located at the intersection of the column and beam mid-line, a special steel cap (2) was placed. In the aforementioned intersection, force transducers (9) were placed. To the side of the force transducer, a steel cantilever was welded. The cantilever had a hole in its centre so the LVDT's pins (8) were held in those places. The steel column caps (2) were fixed in the position by tightening side bolts into the concrete. To fix the frame from translation and rotation, the bottom beam was held by four steel braces (3). Two braces were placed on each face of the beam, underneath the columns. The braces were fixed in place by 4×M20 bolts that were locked to the rails by special tightening system (detail on left of Fig. 5a). Additionally, two steel plates (4) were welded before the front side braces. To tie the opposite braces, two threaded M20 rods were installed. Furthermore, for health and safety reasons as well as for protecting the equipment from possible damage, chains (1) were connected to the crane above and the frame. Two LVDTs were placed horizontally at top of the lower beam, near the columns, and one in the vertical direction in the middle of the lower beam. Their task was to measure possible rotations and torsion. The LVDTs and force transducers were connected to the SIRIUS-HD-16xSTGS data acquisition system (DAQ) with 5 Hz storing speed. The ARAMIS optics were set in front of the test setup, the cameras were adjusted so they could measure depth and plane strains. Note that through this paper there is a reference to the left and right side of the specimens; those refer to the front view perspective (Fig. 5a).

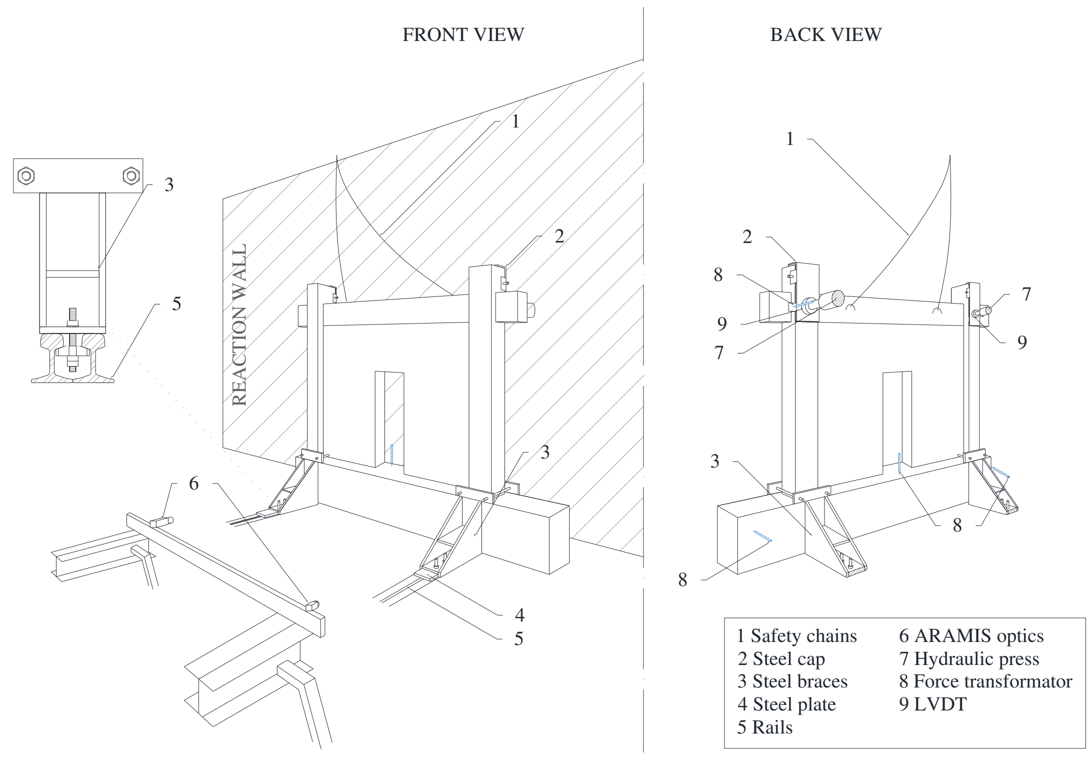

a) Experimental setup scheme

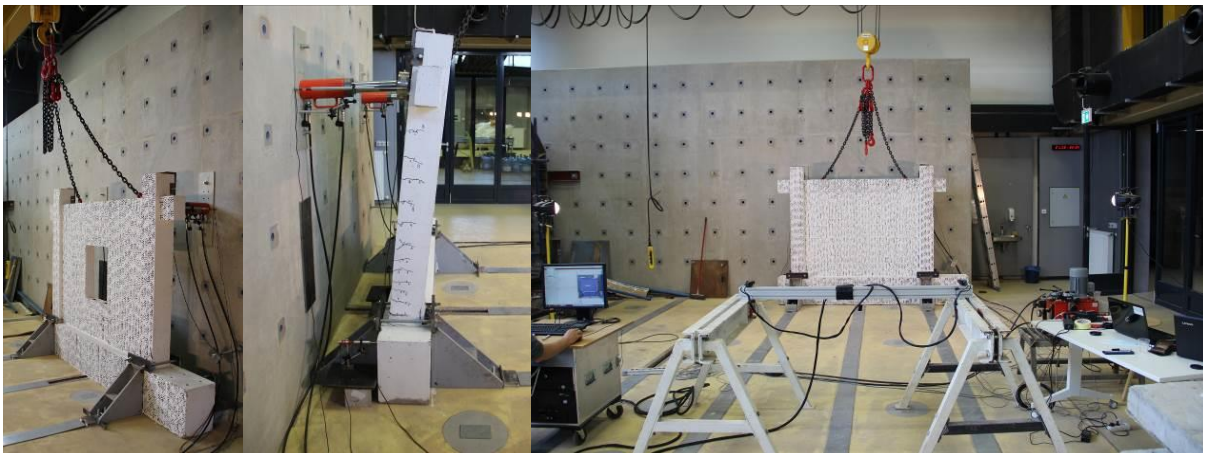

b) Photographs from the experiments
Figure 5. Test setup

Unlike the first test series, this series did not include vertical precompression. The OoP cyclic, quasi-static load was introduced via hydraulic presses. The hydraulic press was operated manually and loaded at increments of 5 kN. The force was repeated twice and was introduced only in one direction. After specimens yielded, the displacement control was restored with increments of 10 mm until the piston reached approx. 150 mm.

3. Results and discussion on OoP tests

3.1 Out-of-Plane cyclic response

The OoP force and displacement/drift ratios were plotted in Figure 6; where the force was the sum from both columns and displacements were an average value between the two upper LVDTs. The recordings from the two lower LVDT's were used to correct the rigid-body movement (RBM) from recorded displacements of the upper LVDTs. It was estimated that the displacements of 1 mm at top of the lower beam correspond to 4.39 mm displacement at the upper beams mid-height. Therefore, Equation 1 was used to correct the displacements (d).

$$d_{\mathrm{corr}} = d_{\mathrm{upper\,LVDT}} - \left(d_{\mathrm{lower\,LVDT}} \cdot 4.39\right) \tag{1}$$

The recording signals were filtered using a *1-D Savitzky–Golay finite-impulse response (FIR)* filter. The filter smooths the data without distorting the signal tendency. This is achieved, by the process known as convolution. That is, by fitting successive subsets of adjacent data points with a low-degree polynomial by the method of linear least squares [29]. The following coefficients were set: length of the filter window = 51; polynomial order = 2; order of the derivative = 0; interpolation mode.

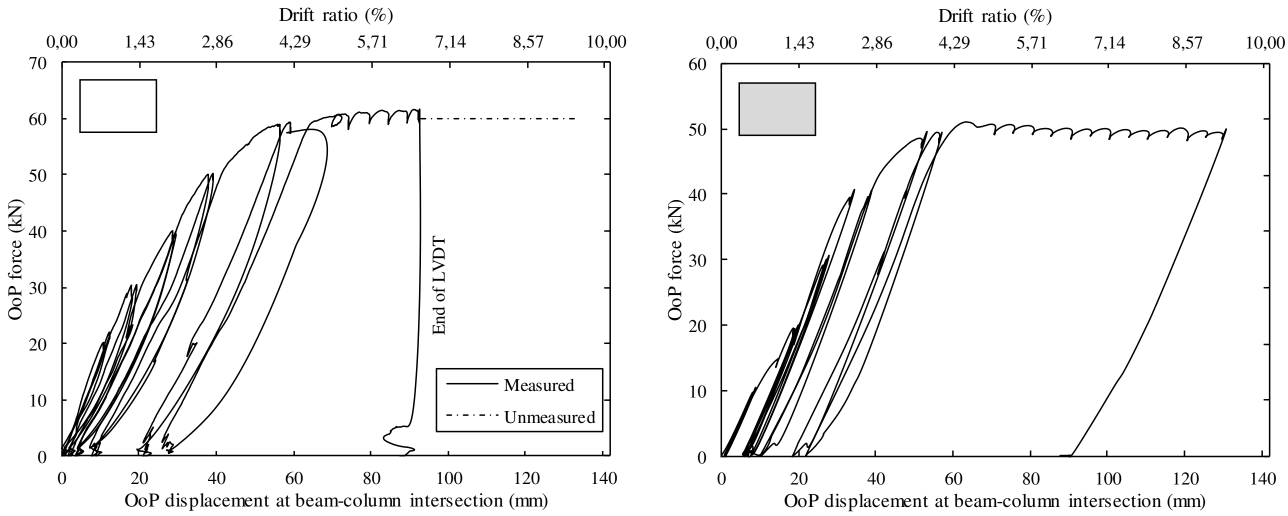

a) BF
b) FI

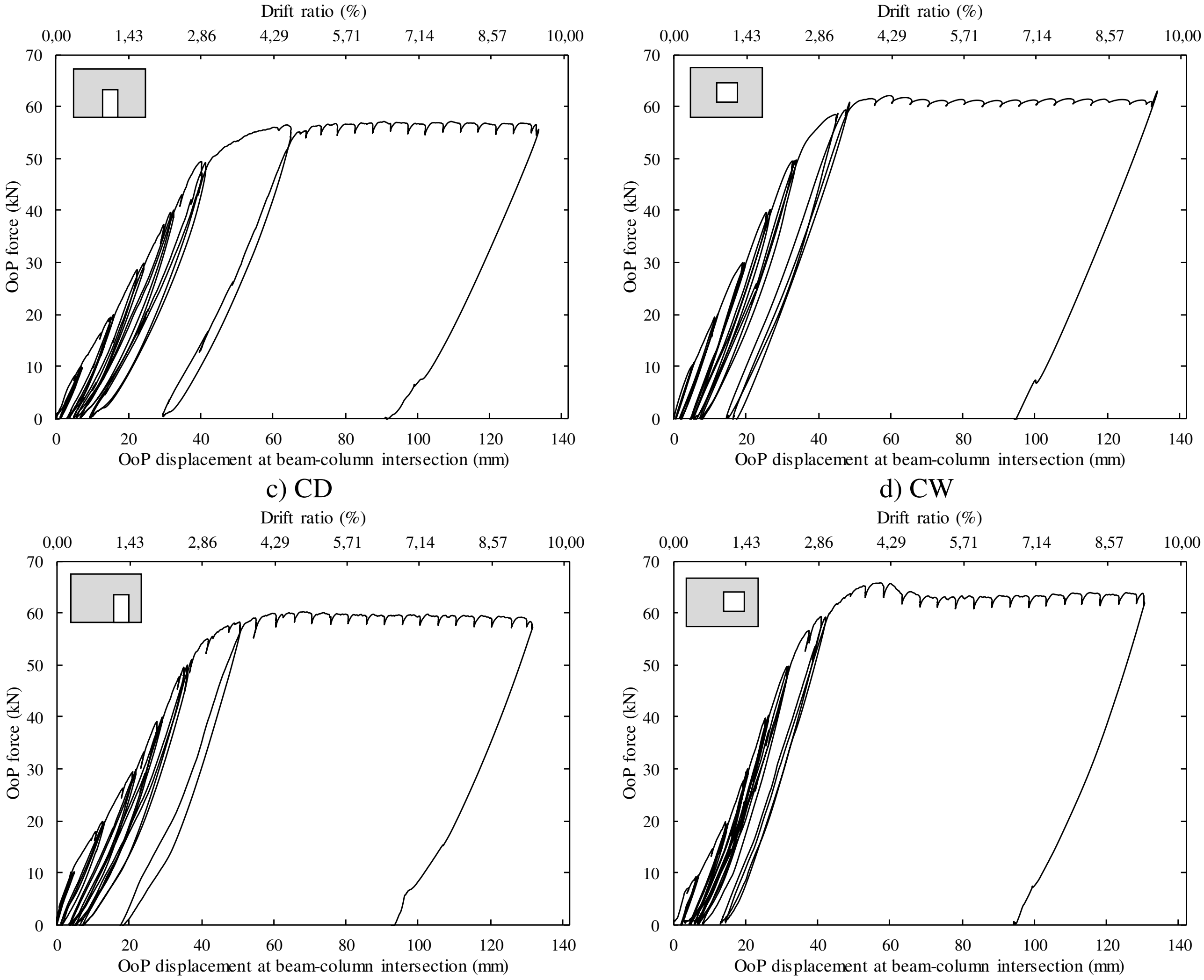

Figure 6. OoP cyclic hysteresis as recorded by the DAQ (corrected for RBM)

When OoP (Fig. 6) are compared to IP hysteresis from the test series described in [24] it was evident that OoP tests had a more linear response. Therefore, there was less energy absorbed by the infill wall, i.e. infill walls and openings, had little effects on the overall behaviour of the specimens. This was also observed in the dynamical test by [30]. Likewise, the hysteresis and their envelopes (Fig. 6 & 10) showed no noticeable differences between each other. Furthermore, all specimens started yielding at an approx. 2.3 % drift ratio, right when the majority of infill walls and the lower beams bedjoint cracking was observed (Fig. 13). Also, all specimens had reached yielding at about 3.6 % drift ratio. The specimens were further subjected to about 9 % drift ratio, when the experiments were stopped as the hydraulics press piston reached its limits. Undoubtedly, the OoP test had exceptional deformation capabilities, due to the dominant cantilever like behaviour.

3.2 OoP unintended torsional effects

The torsional effects were observed both by the DAQ and ARAMIS. These observed by the DAQ, i.e. recorded by LVDTs were plotted in Figure 7. In Figure 7a the *difference trendline* represents the variation tendency of left and right displacement trough time for the EW specimen. In Figure 7b, the distribution of torsional effect, i.e. difference in displacements between the two columns of each specimen was plotted. The points for the calculation of rotation and their differences were presented in Figure 8. The red point in the lower beam was used as an anchor point as it was corrected for RBM. From there the rotations between the points were calculated and then compared with the mirror side of between each other. Note that boxplots in Figure 7b were not corrected for the outliers due to extensive amount of points that are not normally distributed.

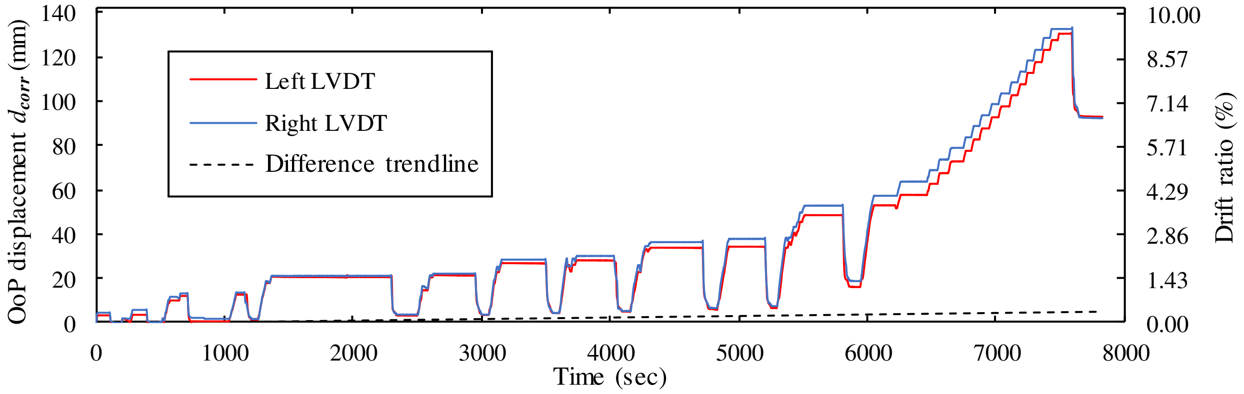

a) Displacement recordings from the upper two LVDTs for the EW specimen

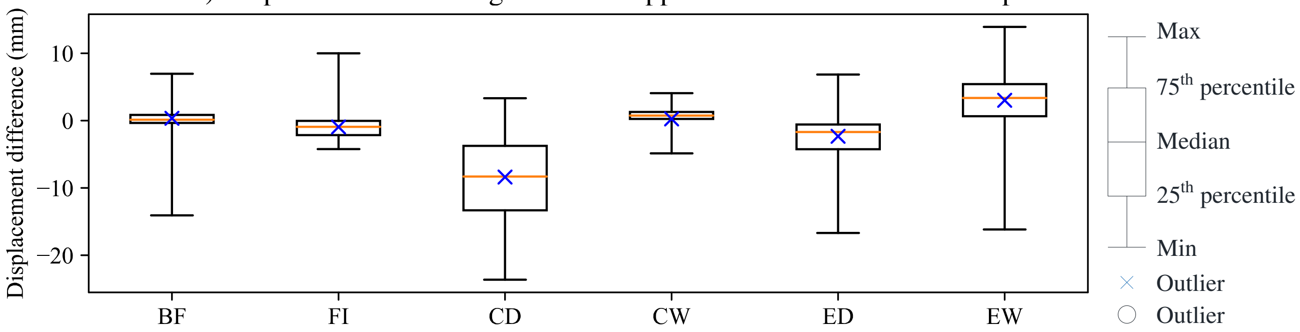

b) Distribution of differences between the upper LVDT readings of each specimen

Figure 7. Accidental torsion described as a difference in displacements of the column LVDTs (RBM corrected)

The unintended torsion was inevitable due to various reasons, the main being: each hydraulic press was operated by hand, force protocol was used, infill walls cracked asymmetrically, however with an insignificant impact. The torsional effects were capture by both DAQ (Fig. 7) in terms of displacement and ARAMIS (Fig. 9) in terms of rotations. It was observed that with the increase of drift ratio the torsional effects increase (Fig. 7a & 8b). The torsional effects vary for each specimen, while some had considerably large peak values. Most of those values were outliers and are results from the last steps of uneven de-loading of the specimens. Yet, the difference in the interquartile range was reasonably small (Fig. 7b & 8b).

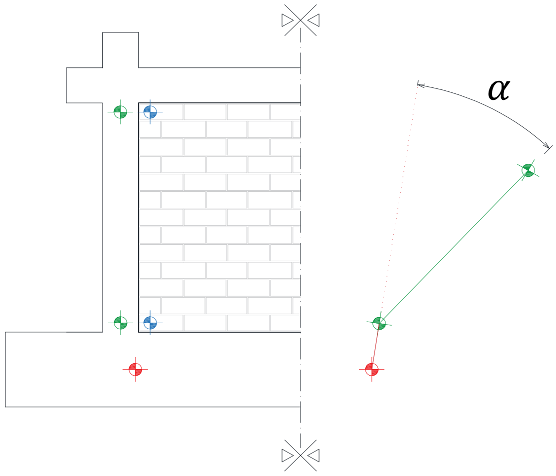

Figure 8. ARAMIS points for rotation (α) calculation

The unintended torsion was additionally examined by the photogrammetry readings and results are shown in Figure 9. Figure 9a shows the differences between the rotation of the CW specimens. In both Figures 9a and 9b, those elements include the difference between the left and right column, opposite strips of the infill wall, and the difference between the average rotation of columns and infill.

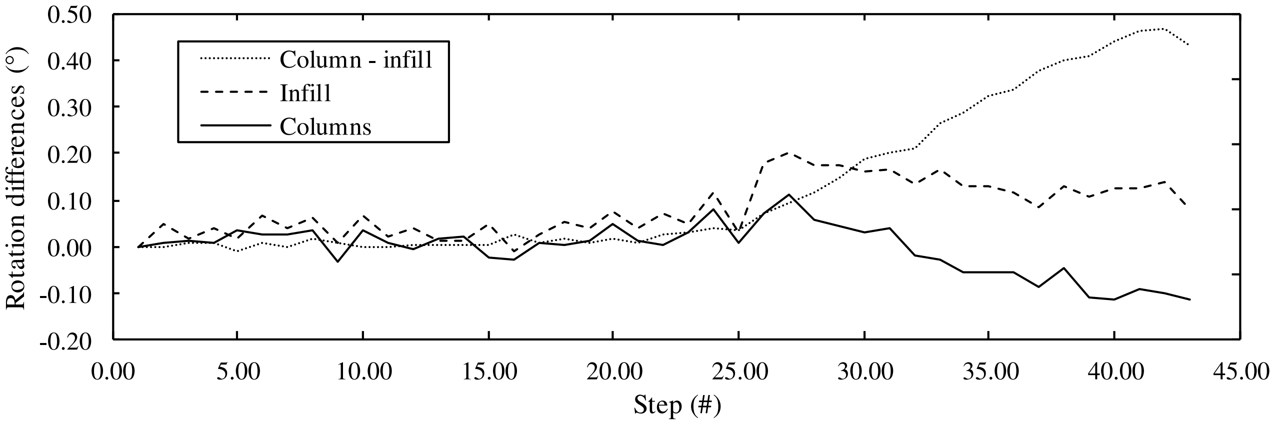

a) Difference in rotations between various elements of the CW model trough protocol steps

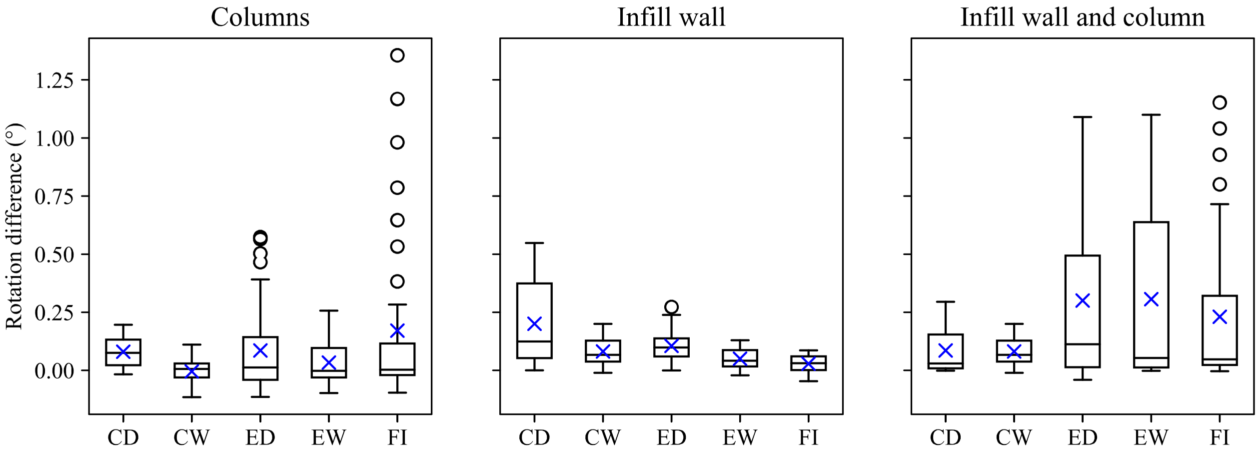

b) Difference distribution of rotations between opposing columns, strips of infill and average column and infill wall rotation (legend as in Fig. 7b)

Figure 9. Accidental torsion described by the difference between rotations of various elements as recorded by ARAMIS (without RBM)

3.3 OoP Capacity Curves

The cyclic envelopes from the OoP tests were plotted in Figure 10. In Figure 10a, the mixed results from both DAQ and ARAMIS are presented. The average displacement between the two columns was recorded and corrected for RBM within ARAMIS's software. The forces transducers were connected to DAQ. Therefore, their values were inputted as an average force of the two columns from readings and multiplied by 2. In Figure 10b, all the envelopes were extracted from signal recordings in Figure 6.

The frame and infill wall interaction was observed in the form of by frame controlled deformation i.e. damage of the infill wall. Optical measurements from ARAMIS photogrammetry provided more insight into the whole topic. The specimens with eccentric openings (ED, EW) had rather small and uniform differences between columns and infill walls rotation prior to the post-yielding region (at about 4 % drift ratio). Afterwards, there was a sizable increase in rotational segregation between the two (Fig. 9a & right boxplot of Fig 8b). This could be handed to the fact that at such high drift ratios, the infill wall debonds from the frame (Fig. 13) and nearly all bedjoints on the shorter side of the wall next to the openings cracked (Fig. 12e & f). The same was not observed for other specimens. In other respects, the infill wall and frame overall behaved as a single unit (Fig. 14 @ OoP displacements), also observed in dynamical OoP tests by [31,32]. The highest strains across the specimens were noticed in the infill wall mostly near the columns; hence column – infill wall separation (Fig. 9), and on the bedjoints. While on the frame, near the bottom.

The differences between the cyclic envelopes from Figure 10a and b are presented in Figure 11. Figure 11 was divided into two pieces, one showing mean absolute error (MAE) of all combined specimens for every + 0.5 % drift ratio; while other, the MAE by specimen considering all drift ratios. The MAE was calculated using Equation 2, where the points for the drift ratios were obtained via linear interpolation.

$$\text{MAE} = \frac{1}{n}\sum_{j=1}^{n}\left|W_j - \hat{W}_j\right| \tag{2}$$

Where: W is OoP force with index referring to data logger; n is the number of elements.

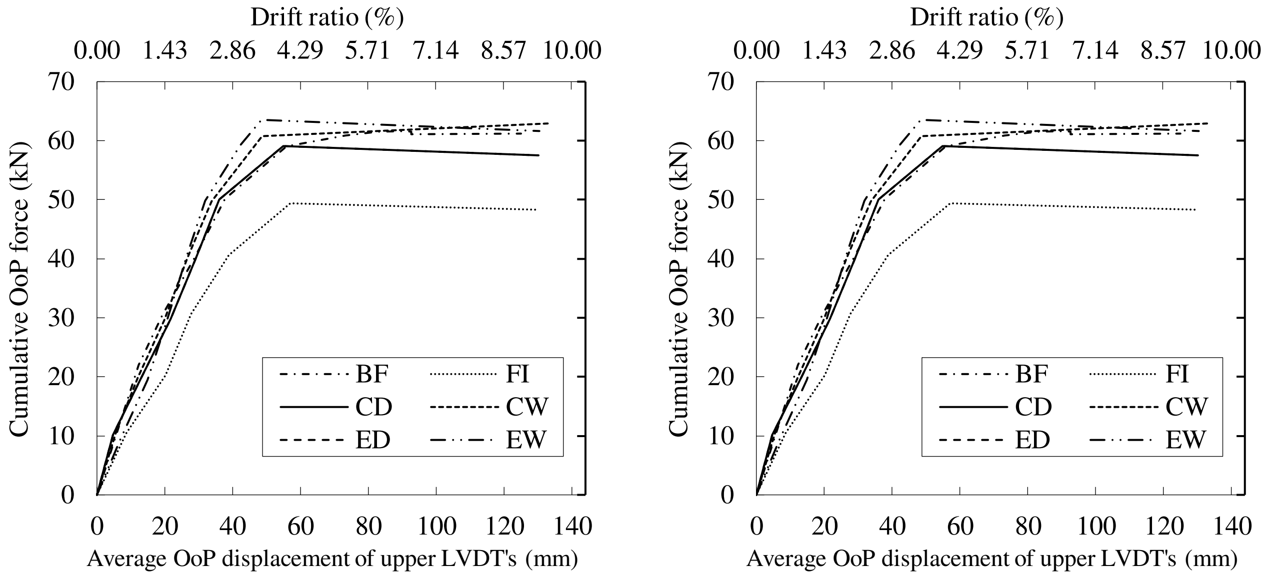

a) Displacement records by ARAMIS force by DAQ

b) Records from DAQ

Figure 10. OoP cyclic envelopes as assembled different devices

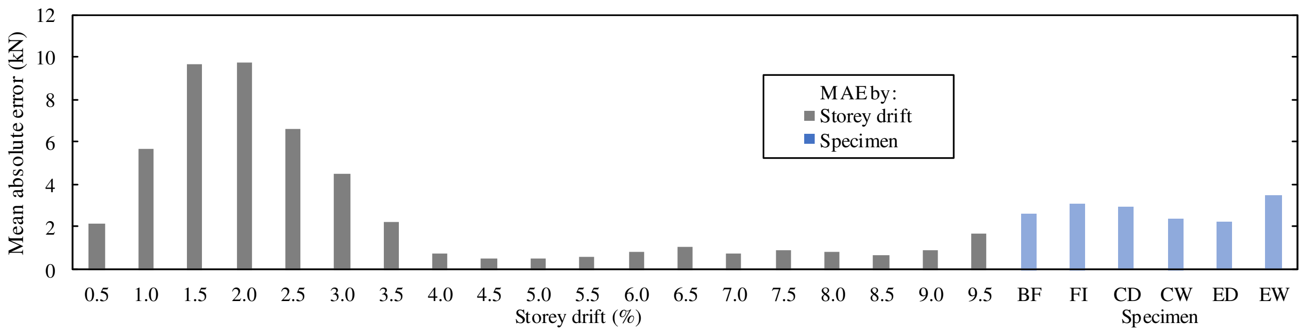

Figure 11. MAE difference between cyclic envelopes

3.4 OoP Cracks and Damage Occurrence

The crack patterns were plotted in Figure 12, for back (tensile) face and front (compressive) face, respectively. Additionally, the side view of column's crack pattern is shown. In overall, as shown in Figure 12, the back (tensile) face revealed large amount of horizontal bending cracks throughout the length of the wall and in the columns, irrespective of the opening size, type and position. At the front (compressive) face only the spalling of concrete at column feet was observed.

The crack occurrences by drift ratio/displacement are shown in Figure 13. Figure 13 has mapped all the cracks and their occurrences from all the tested specimens. The cracks were mapped for every load step until yielding was reached.

Fist cracks on the specimens were observed on the lower parts of the columns, as expected from the cantilever mechanics and the development of plastic hinges. The cracking of the infill wall started at about 1.25 – 2.00 % drift ratio, with the outlier of the EW specimen that cracked at 0.75 % drift ratio. Nearly all the recorded cracks were those of bedjoints. Most of the headjoint cracks were the result of debonding of infill wall and columns, while there were very few headjoints cracked between the blocks. Also, nearly no cracking of the blocks was observed. All initial cracks on the infill walls were located on bedjoints between lower two rows of the block, with 3/5 of those additionally included headjoint cracks between infill walls and each of the columns (Fig. 13). The infill walls and columns debonding occurred in the range of about 1.25 – 2.25 % drift ratio with the outlier of the CD specimen that parted at about 2.80 % drift ratio. Similarly, the debonding of the infill wall and lower beam occurred in a range of about 1.25 to 2.50 % drift ratio. Due to the nature of one-directional loading, the front side of the specimen suffered from compression stress, mostly observed as the crushing of the column's lower parts (Fig. 12). However, in the case of both the CW and EW specimens containing window openings (Fig. 12d & f), there was cracking of the infill walls frontal, i.e. compression side. Whereas, the EW specimen had also visible debonding of the infill wall and both columns. For the most part, the infill wall had predictable bending crack modes similar to those observed on the wall's pure bending test with load parallel to bedjoints [27]. The crack patterns of the FI and specimens with centrally aligned openings had a more or less symmetrical pattern.

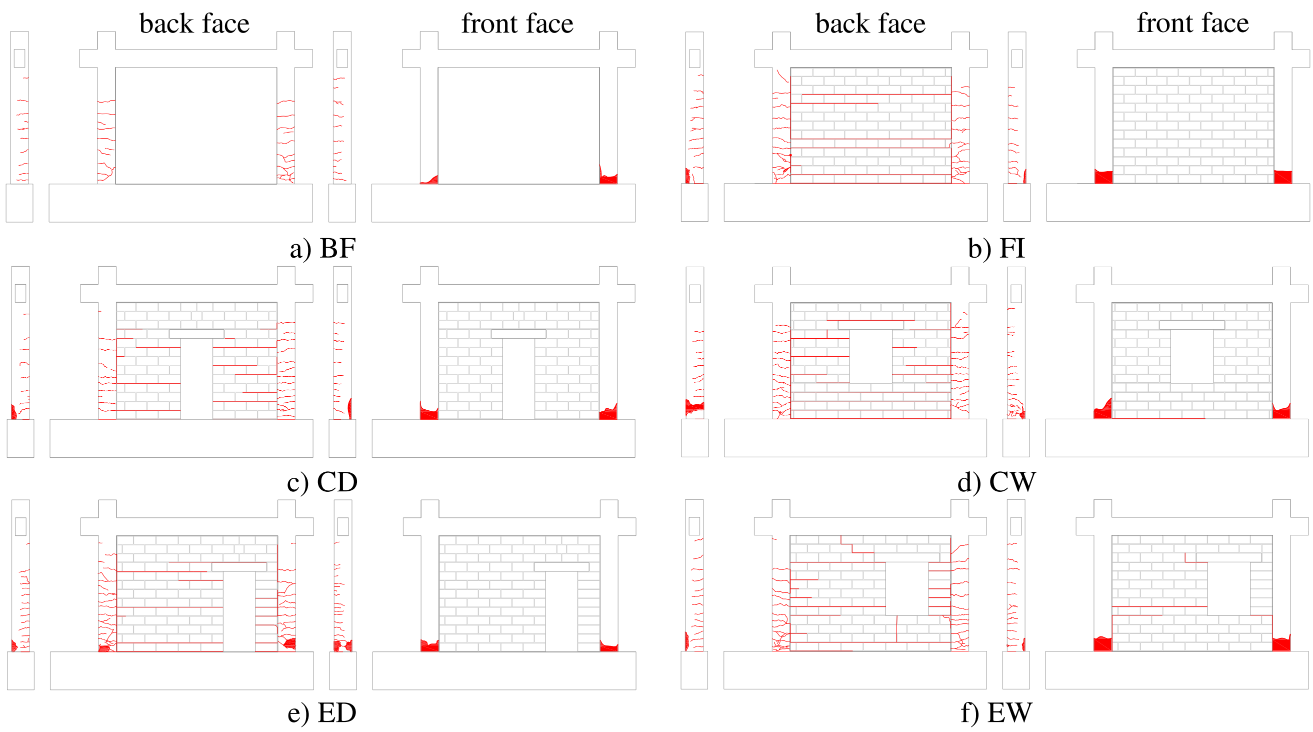

Figure 12. Final crack patterns

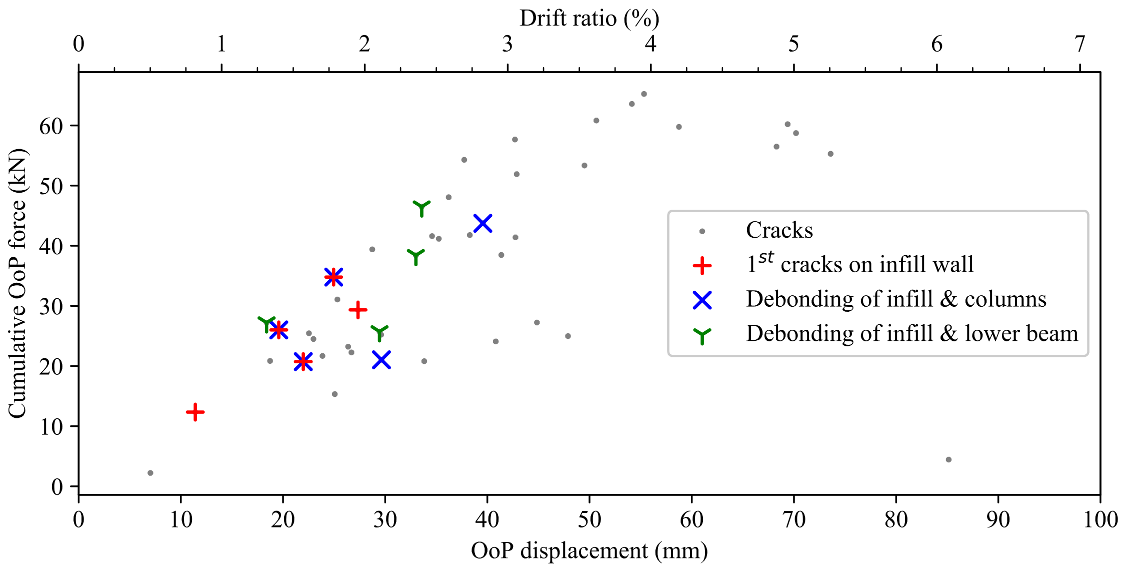

Figure 13. Crack occurrences by drift ratio

To the contrary, the ED and EW specimens with eccentrically positioned openings had uneven cracking. More bedjoints cracked on the shorter side of the wall next to the opening. The damages were comparatively greater in specimens with openings than the fully infilled frame. The horizontal cracks in line with the openings spreaded to the wall sides. The infill detached from the frame creating loose on one side and non-existing restrain condition on the other side (opening). Therefore, the infill walls with openings were disjointed in more ways than the fully infilled one. In other respects, the subjacent bedjoint cracking was also observed in the drift force test from [8,21] (Fig. 2). However, the specimens were subjected to a comparatively low drift ratio of 1.7 %. By the same token, the crack patterns were also similar to those of dynamical tests from [31,32].

OoP displacements as well as von Mises strains captured by optical measurements were presented in Figure 14. The colour bars of figures with OoP displacements are presented in millimetre (mm) units, while those of von Mises strains multiplied with 100 i.e. expressed in (%). The hollow clay blocks had uniquely different mechanical characteristics in- and perpendicular to the direction of voids (Tab. 2). Therefore, the von Mises strain was used in order to observe the strain changes through the specimen and not for the sake of reporting their values. The BF specimen has only OoP displacements as the focus of this paper was on the infill. Furthermore, Figures 14g and 14i have concentrations of strains visible between the left column and infill. Other figures depicting strains also have them on some parts of specimen outlines.

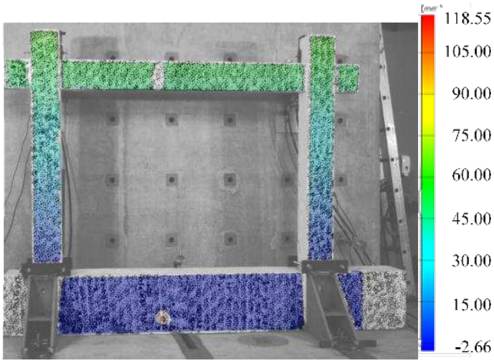

BF: OoP displacements

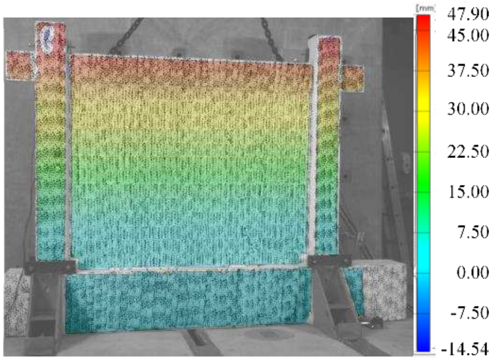

b) FI: OoP displacements

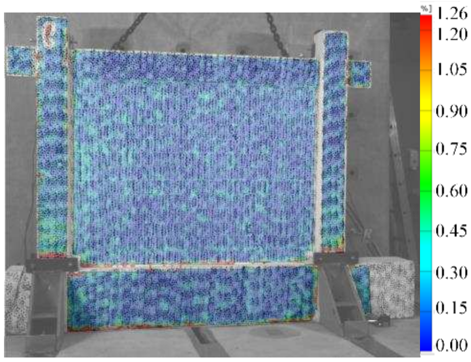

c) FI: von Mises strain

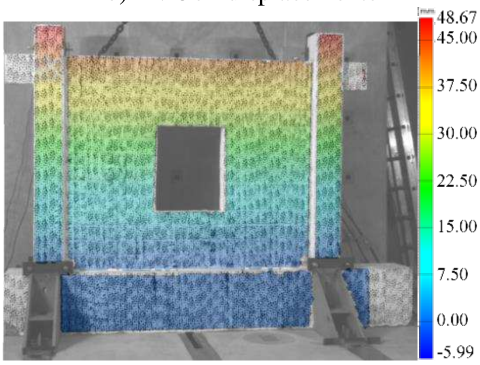

d) CW: OoP displacements

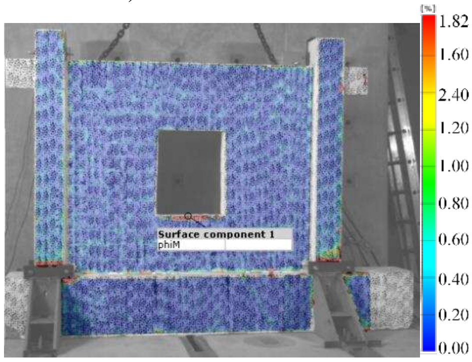

e) CW: von Mises strain

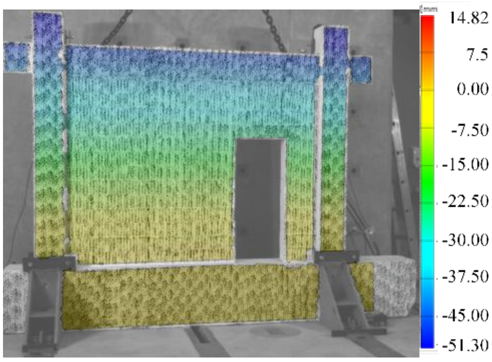

f) ED: OoP displacements

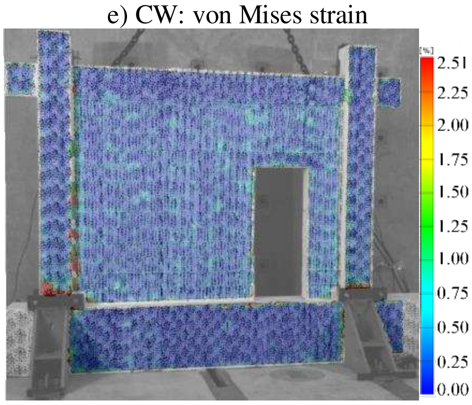

g) ED: von Mises strain

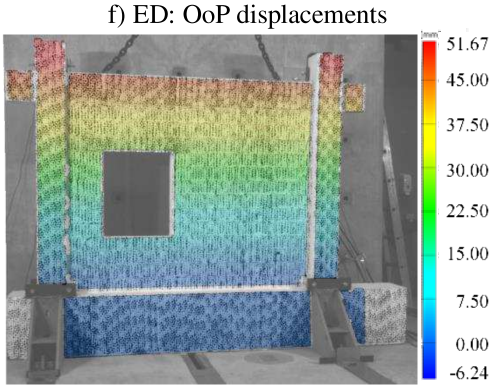

h) EW: OoP displacements

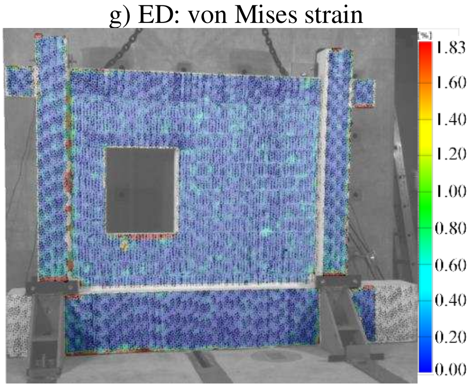

i) EW: von Mises strain

Figure 14. Optical measurements result at the point of specimen yielding occurrence

Though the aforementioned dynamical tests also developed plastic hinges and with it cracks on top of columns, and the upper parts of the infill wall. This is the result of having both vertical precompression and elastically clamped column and beam ends due to RC slabs with additional loads. For the same reason, [31] observed; for the sake of terminology: a two-hinged arching action. More precisely, clamping of opposite ends of the infill wall. Consequently, due to having no restraining conditions on the top part of the specimens, both experiments presented in this paper and those of [21] did not develop any arching action.

4. Conclusions

The presented experimental campaign was a part of a test series that included medium ductility class reinforced concrete frames with unreinforced masonry infill walls. The first test series included in-plane, while the one presented here, out-of-plane tests. The out-of-plane drift loading had one-directional cyclic, quasi-static force governed protocol. The protocol had a step load of 5 kN repeated twice until the plastic behaviour was reached. Afterwards, the displacement governed protocol was used with + 5 mm steps. The experimental setup consisted of 6 specimens: a bare frame; fully infilled frame, frame with infill wall and centrally positioned door opening; frame with infill wall and centrally positioned window opening; frame with infill wall and eccentrically positioned door opening and finally; frame with infill wall and eccentrically positioned window opening.

The test had two monitoring systems. Whereas, one had physical data acquisition, with the force transducers and linear-variable differential transducers. And the other, optical measurements of the frontal, i.e. compressive sides of the specimens. The two were comparatively similar in terms of specimen's behaviour. Accidental torsion was recorded by both and was an inevitable occurrence due to several causes; e.g. the two hydraulic presses were controlled separately by hand, uneven cracking, force protocol, etc. Additionally, ARAMIS captured that the specimen as a whole behaves as a single unit as the same was found in other dynamical studies. Additionally, within the plastic region (> 4 % drift) specimens with eccentric openings developed a distinct separation of rotational capabilities between the frame and the infill wall. Both systems captured rigid-body movement mostly as a rotation of the whole specimen. The rotation was measured at the upper end of the lower beam where the values were small, however, the same magnified when examining the displacements at the upper beams mid-height. All the displacements/storey drifts were corrected for this effect.

Regarding the overall behaviour of specimens, the role of infill walls and openings had an insignificant role. This was examined in several points, main being: the out-of-plane hysteresis had more linear response than the in-plane ones, hence, there was less energy absorbed by the infill walls; the hysteresis and their envelopes were similar in terms of load-bearing capacity, initial stiffness's, yield points; crack occurrences, etc. Nevertheless, when the infill wall was examined independently and it was found that it could develop heavy damage and pose life and property danger.

The tests exhibited abundantly high stability, endured storey drifts up to approx. 9 %. This can be attributed to the matter that: the specimens were subdued to one-way loading; there was no gravity load; moment-resisting frames were subjected to cantilever-column like mechanics. Infill walls with openings had accumulated more damage than the plain infill wall, especially those with eccentrically positioned openings. Moreover, the openings rendered the infill walls restrain conditions considerably looser, and with it more hazardous. Infill walls collectively started cracking at a storey drift ratio of about 1.25 %, the separation from the frame mostly occurred around 1.25 – 2.25 % as detachment from columns; similarly, detachment from the lower beam at about 1.25 – 2.50 %. Therefore, it is expected that the infill wall with consideration of openings withstands light damage up to a 1.25 % storey drift, from 1.25 – 2.00 % heavy but usable damage and > 2.00 % heavy but unusable damage. The provided limits are within the scope of Eurocode 8's [33] limit of 2.5 % storey drift, when non-structural (e.g. infill walls, partitions, plumbing, etc.) damages risk the safety of life and property.

The dynamical tests [31,32] observed that the infill wall and the frame move together as a single unit, even though infill walls possessed higher acceleration. Thus, a change of restrain conditions during an earthquake event would result in disjointed movement between the frame and infill wall that could cause inertial failure due to infill walls accelerated mass. A similar sequence of events was observed in A1 specimen from [31] dynamical tests when the infill wall lost its restrain with the upper beam causing part of it to fall out. Notice that this has occurred even though [11] observed arching action was achieved even with dry-stacked masonry. Furthermore, the loss in restrain conditions could potentially affect the behaviour of overall structure with combined in- and out-of-plane loading scenarios. Note that the out-of-plane storey drift loading did not affect in-plane performance in [34] research; however, the study pushed the frame up to 1.7 % drift ratio and no cracks with surrounding frame except the infill wall and lower beam one did occurred.

Acknowledgments

The research presented in this article is a part of the research project FRAmed-MAsonry composites for modelling and standardization [HRZZ-IP-2013-11-3013] supported by Croatian Science Foundation and its support is gratefully acknowledged.

Advice given by Prof. Roko Žarnić from University of Ljubljana, Slovenia, has been a great help in the adoption of the experimental approach proposed herein.

References

[1] G. E. Howe, Behavior of non-loadbearing block walls under wind loading, Reprinted by American Institute of Steel Construction, Inc., New York, U.S.A. (1936).

[2] CEN, Eurocode 8: Design of Structures for Earthquake Resistance - Part 1: General Rules, Seismic Actions and Rules for Buildings (EN 1998-1:2004), European Committee for Standardization, Brussels, 2004.

[3] E.L. McDowell, K.E. McKee, E. Sevin, Arching Action Theory of Masonry Walls, J. Struct. Div. 82 (1956) 1–8.

[4] B. Gabrielsen, C. Wilton, Shock tunnel tests of arched wall panels, (1974). http://www.dtic.mil/docs/citations/ADA006682 (accessed June 8, 2018).

[5] M. Lew, D.A. Friedman, W.A. Anderson, D.A. Friedman, L.T. Tobin, I. Wong, 2011 Annual Meeting Highlights Chang ' s Distinguished Lecture on Dynamics of Urban Earthquake Risk, EERI Newsl. 45 (2011) 12.

[6] W. Jäger, T. Vassilev, J. Hoffmann, P. Schöps, Unreinforced masonry basement walls - a comparison of theoretical design approach es and numerical simulations, in: 14th Int. Brick Block Mason. Conf., Sydney, Australia, 2008. http://www.hms.civil.uminho.pt/ibmac/2008/14IBMAC_189.pdf.

[7] R. Flanagan, R. Bennett, Bidirectional behavior of structural clay tile infilled frames, J. Struct. Eng. 125 (1999) 236–244. https://doi.org/10.1061/(ASCE)0733-9445(1999)125:3(236).

[8] R. Henderson, W. Jones, E. Burdette, M. Porter, The effect of prior out-of-plane damage on the in-plane behavior of unreinforced masonry infilled frames, in: Fourth DOE Nat. Phenom. Hazards Mitig. Conf., 1993: p. 18. https://www.osti.gov/scitech/biblio/10107474 (accessed March 19, 2018).

[9] F. Anić, D. Penava, L. Abrahamczyk, V. Sarhosis, A review of experimental and analytical studies on the out-of-plane behaviour of masonry infilled frames, Bull. Earthq. Eng. 18 (2020) 2191–2246. https://doi.org/10.1007/s10518-019-00771-5.

[10] C.B. Monk, Resistance of structural clay masonry to dynamic forces: a design manual for blast resistance, Struct. Clay Prod. Res. Found. 7 (1958).

[11] R. Angel, D.P. Abrams, D. Shapiro, J. Uzarski, M. Webster, Behavior of reinforced concrete frames with masonry infills, University of Illinois Engineering Experiment Station. College of Engineering. University of Illinois at Urbana-Champaign., 1994.

[12] F. Akhoundi, G. Vasconcelos, P. Lourenço, Experimental Out-Of-Plane Behavior of Brick Masonry Infilled Frames, Int. J. Archit. Herit. 14 (2020) 221–237. https://doi.org/10.1080/15583058.2018.1529207.

[13] S. Hak, P. Morandi, G. Magenes, Out-of-plane Experimental Response of Strong Masonry Infills, in: 2nd Eur. Conf. Earthq. Eng. Seismol., Istanbul, Turska, 2014.

[14] A. Furtado, H. Rodrigues, A. Arêde, H. Varum, Experimental Characterization of the In-plane and Out-of-Plane Behaviour of Infill Masonry Walls, Procedia Eng. 114 (2015) 862–869. https://doi.org/10.1016/j.proeng.2015.08.041.

[15] P. Ricci, M. Di Domenico, G.M. Verderame, Experimental assessment of the in-plane/out-of-plane interaction in unreinforced masonry infill walls, Eng. Struct. 173 (2018) 960–978. https://doi.org/10.1016/j.engstruct.2018.07.033.

[16] I.S. Misir, O. Ozcelik, S.C. Girgin, U. Yucel, The Behavior of Infill Walls in RC Frames Under Combined Bidirectional Loading, J. Earthq. Eng. 20 (2016) 559–586. https://doi.org/10.1080/13632469.2015.1104748.

[17] D.P. Abrams, R. Angel, J. Uzarski, Out-of-Plane Strength of Unreinforced Masonry Infill Panels, Earthq. Spectra. 12 (1996) 825–844. https://doi.org/10.1193/1.1585912.

[18] A. Furtado, H. Rodrigues, A. Arêde, H. Varum, Effect of the Panel Width Support and Columns Axial Load on the Infill Masonry Walls Out-Of-Plane Behavior, J. Earthq. Eng. (2018) 1–29. https://doi.org/10.1080/13632469.2018.1453400.

[19] C. Wang, Experimental investigation on the out-of-plane behaviour of concrete masonry infilled frames, Dalhousie University, 2017.

[20] R. Sepasdar, Experimental investigation on the out-of-plane behaviour of concrete masonry infilled RC frames, Dalhausie University, 2017. http://dalspace.library.dal.ca/handle/10222/72875.

[21] R.D. Flanagan, Behavior of structural clay tile infilled frames, Tennessee, USA, 1994.

[22] F. Anić, D. Penava, L. Abrahamczyk, V. Sarhosis, Computational Evaluation of Experimental Methodologies of Out-of-Plane Behavior of Framed-Walls with Openings, Civ. Eng. J. (2018).

[23] D. Penava, Influence of Openings on Seismic Behavior of Reinforced Concrete Frames with Masonry Infill Walls (in Croatian: Utjecaj otvora na seizmičko ponašanje armiranobetonskih okvirnih konstrukcija sa zidanim ispunom), Josip Juraj Strossmayer University of Osijek, PhD Thesis. (2012).

[24] V. Sigmund, D. Penava, Influence of openings, with and without confinement, on cyclic response of infilled R-C frames - An experimental study, J. Earthq. Eng. 18 (2014). https://doi.org/10.1080/13632469.2013.817362.

[25] CEN, Eurocode 6: Design of masonry structures - Part 1-1: General rules for reinforced and unreinforced masonry structures (EN 1996-1-1:2005), European Committee for Standardization, Brussels, 2005.

[26] British Standard Institute, BS EN 1504-3: Products and systems for the protection and repair of concrete structures. Definitions, requirements, quality control and evaluation of conformity. Structural and non-structural repair, 2005.

[27] F. Anić, D. Penava, D. Varevac, V. Sarhosis, Influence of Clay Block Masonry Properties on the Out-of-Plane Behaviour of Infilled RC Frames, Teh. Vjesn. (2018).

[28] MAPEI, MAPEGROUT T60 techincal details, 2020. https://www.mapei.com/it/en/products-and-solutions/products/detail/mapegrout-t60.

[29] A. Savitzky, M.J.E. Golay, Smoothing and Differentiation of Data by Simplified Least Squares Procedures, Anal. Chem. (1964).

https://doi.org/10.1021/ac60214a047.
[30] R.C. Henderson, M.L. Porter, W.D. Jones, E.G. Burdette, Influence of prior out-of-plane damage on the in-plane behavior of masonry infilled frames, TMS J. 24 (2006) 71–82.
[31] Y.H. Tu, T.H. Chuang, P.M. Liu, Y. Sen Yang, Out-of-plane shaking table tests on unreinforced masonry panels in RC frames, Eng. Struct. (2010). https://doi.org/10.1016/j.engstruct.2010.08.030.
[32] J.J. Fowler, Analysis of dynamic testing performed on structural clay tile infilled frames, Oak Ridge, TN (United States), 1994.
[33] CEN, Methods of Test for Masonry - Part 1: Determination of Compressive Strength (EN 1052-1:2004), European Committee for Standardization, Brussels, 1998.
[34] R.D. Flanagan, Behavior of structural clay tile infilled frames, Oak Ridge, Tennessee, 1994.